

Dependence of the morphology of polymer dispersed liquid crystals on the UV polymerization process

S. A. Carter,^{a)} J. D. LeGrange,^{b)} W. White, J. Boo, and P. Wiltzius

Bell Laboratories, Lucent Technologies, 600 Mountain Avenue, Murray Hill, New Jersey, 07974

(Received 17 October 1996; accepted for publication 15 January 1997)

Using confocal microscopy, we have studied the morphology of polymer dispersed liquid crystals (PDLC) as a function of polymer/liquid crystal composition, polymer cure temperature, and ultraviolet (UV) curing power and determined how this morphology affects the electro-optical properties. The PDLC morphology consists of a spongelike texture where spherically shaped liquid crystalline domains are dispersed in a polymer matrix. These domains grow as the fraction of liquid crystal increases and as the UV curing power decreases. We observe no significant changes in domain size with changes in the curing temperature. Instead, high-temperature cures result in coalescence and the formation of elliptical-shaped liquid crystal domains. The temperature at which this coalescence starts to be observed marks a threshold temperature T_{th} , above which the switching properties are strongly dependent on morphology. Below T_{th} the switching properties are largely independent of morphology. © 1997 American Institute of Physics. [S0021-8979(97)05508-4]

INTRODUCTION

Polymer dispersed liquid crystals (PDLCs) are promising materials for reflective and projection displays, window shutters, and holographic recording media¹⁻⁴ due to their relatively low cost and ease of processing over other technologies. PDLCs consist of a homogeneous mixture of liquid crystal and monomer in which phase separation has been induced by either thermal curing, UV curing, or solvent evaporation. For polymer/liquid crystal compositions relevant for display applications, the polymerization of the monomer causes the liquid crystal to phase separate into “droplets” or domains separated by the polymer matrix. The nematic texture within these domains is randomly oriented with respect to the neighboring domains such that incoming light into the cell is scattered, and the PDLC appears white. When an electric field is applied across the cell, the liquid crystal domains align, and the PDLC is transparent if the ordinary index of refraction is matched to the index of the polymer. The voltage V and speed τ at which the PDLC switches from whiteness to transparency and the optical contrast between the white and transparent state is controlled by the size, shape, and anchoring energy of the liquid crystal domains, as well as the dielectric anisotropy and viscosity of the liquid crystal (LC). While the latter properties depend on the selection of the liquid crystalline material, the former properties depend on the liquid/crystal monomer composition and the method of polymerization.

Several investigations^{5,6} into the phase diagram of the PDLC mixture have shown that the phase separation occurs along a line in temperature-composition space (Fig. 1). Before polymerization the system consists of a homogeneous mixture of monomer and LC. The isotropic phase occurs at conditions above this line, and a phase separated mixture of nematic LC-rich and isotropic monomer-rich regions below

it. When polymerization is initiated in the homogeneous state, the growth of the polymer matrix results in an increase in temperature of the phase separation line. Phase separation into LC-rich domains occurs when the polymerization has progressed far enough such that the cure temperature of the PDLC mixture matches the temperature of this phase separation line T_{ps} . At this point, nucleation of LC domains is initiated and the LC domains start to grow. There are several time scales that are important for determining the PDLC morphology: the time it takes for the drops to grow to their space limited size via molecular diffusion; the time it for the drops to coalesce via the movement of polymer matrix from between neighboring droplets; the time for coalesced droplets to relax into spherical domains; and the time for the polymer matrix to sufficiently solidify to retard droplet and matrix movement.⁶ Extracting these time scales is difficult since they themselves are time dependent and depend on the extent of the phase separation process. In a simplified approach, one can assume that the rate of solidification can be controlled by the UV curing power, with lower power resulting in larger droplets, and by the extent of polymerization at the phase separation point, with lower compositions and higher temperature resulting in a larger polymer matrix when phase separation is initiated and subsequently smaller droplets. In contrast, the coalescence of the LC droplets, which is determined in part by the viscosity of the polymer matrix, will cause higher temperatures (lower viscosity) to result in more coalescing and larger droplets. The PDLC morphology should be largely determined by the mechanism for nucleation of the liquid crystal domains and the competition between these time scales.

In this article we attempt to deconvolute the importance that these effects have in determining the morphology of a PDLC. We study compositions with foam-type morphology (~80% LC) where the light scattering occurs primarily among droplets, rather than that between LC and matrix, leading to a reduction in scattering at larger angles. Our methodology is to fix the monomer polymer viscosity by fixing temperature, and then control the extent of polymer-

^{a)}Currently at Physics Department, University of California, Santa Cruz, CA 95064.

^{b)}Electronic mail: jdl@lucent.com

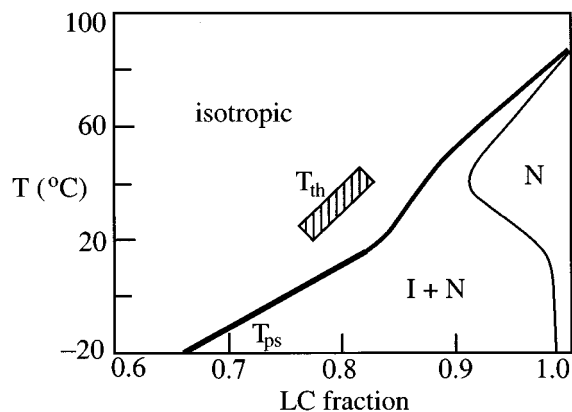


FIG. 1. Binary phase diagram for TL205/PN393 LC/polymer mixtures, where *I* is isotropic and *N* is nematic. The coexistence curves prior to photopolymerization are indicated by solid black lines. As polymerization proceeds, the coexistence curves move to higher temperatures and lower LC fraction. T_{ps} is the temperature at which the phase separation into nematic-rich LC droplets and isotropic-rich polymer occurs. The hatched region T_{th} is the threshold cure temperature at which the droplets start to coalesce.

ization at the phase boundary and the rate of polymerization by varying composition and UV cure power, respectively. In addition, we change the polymer matrix/LC viscosity and the extent of polymerization at the phase boundary by fixing the composition and curing power and curing at different temperatures. In the former experiments, we observe large changes in the morphology which can be explained by the simplistic model described above. However, contrary to expectations, we observe that the drop size does not significantly change with increasing cure temperature. Instead, increasing cure temperatures cause the droplets to coalesce to form elliptical shaped domains which become larger spherical domains at sufficiently high temperatures. We discuss possible mechanisms for the formation of these morphologies and compare the morphology to the electro-optic properties.⁷

EXPERIMENTAL METHODS

The PDLC cells were assembled in a clean room using large glass plates, $420 \times 300 \text{ mm}^2$, coated with indium-tin-oxide (ITO) and separated by $8 \mu\text{m}$ spherical spacers made of plastic. For the microscopy measurements, a $175\text{-}\mu\text{m}$ thick ITO-coated glass plate was used as the top plate since the confocal microscope used for the measurements had a $200 \mu\text{m}$ focal range. The two plates were sealed under vacuum using a UV curable glue.⁷ The resulting cell gap was $13.0 \pm 4.0 \mu\text{m}$ due to the flexibility of the top plate. Measurements of cell gap over a single cell showed that the gap was uniform to within 15%. Repeated measurements showed that the morphology was not affected by the variances in the gap.⁸ The PDLC mixture consists of an acrylate based monomer mixture (Merck PN393) and a superfluorinated LC mixture (Merck TL213) where the LC fraction was varied between 76% and 82%. The 82% mixture had an average phase separation temperature of 15°C which decreased with decreasing LC fraction as shown in Fig. 1. A fluorescent probe (Exciton Corporation), pyromethene 580, of weight fraction

in the range of 10^{-4} – 10^{-3} was added to this mixture. This probe dissolved preferentially into the monomer enabling good optical contrast between the LC and polymer. The cells were filled by capillary forces and then UV cured on a temperature controlled plate at temperatures in the range of 10 – 48°C . The UV lamp power was varied from $22 \mu\text{W}/\text{cm}^2$ to $16 \text{mW}/\text{cm}^2$ using neutral density filters. In all cases, phase separation occurred within 20 s of UV exposure; nonetheless, the cells were cured for 400 s to ensure that the polymer matrix was completely cross linked.

The PDLC morphology was determined using a commercial fluorescent confocal microscope with a resolution of $0.4 \mu\text{m}$. A 60 Hz voltage source was used to switch to the transparent (on) state of the PDLC cell, sufficiently reducing the light scattering so, that three-dimensional scans through the entire thickness of the PDLC cell could be obtained. We observed that the PDLC morphology does not depend on cell thickness, except at distances roughly within 1 – $2 \mu\text{m}$ of the two plates (Fig. 2 and Fig. 6 below). Measurements, therefore, were typically obtained at a depth of 3 – $4 \mu\text{m}$ below the top plate. Switching voltage, switching speed, and standardized luminance (the reflectivity of white light normalized to a 40% brightness standard) were measured using a normal viewing angle display measurement system (Autronic-Melchers DMS-703) on both the microscopy cells and standard thick glass cells prepared under the same conditions in order to verify consistency.⁷ In some cases the switching voltages and luminance had to be adjusted for the differences in gap size. The fluorescent probe did not affect the electrical properties in the range of concentrations used in the experiment. At concentrations near 10^{-3} , a slight orange coloring of the PDLC cells occurred, making it necessary to correct the measured values of luminance (by an offset $<15\%$) in order to match the standardized cell prepared at the same conditions without the probe.

RESULTS

In Fig. 3 the morphology of PDLCs cured at room temperature and at $16 \text{mW}/\text{cm}^2$ lamp power is shown as a function of LC fraction between 76% and 82%. Below 76% the LC domains are no longer clearly discernible within the resolution of the microscope. The morphology consists of sponge- or foamlike texture where the LCs form closely packed spherical domains within the polymer matrix. This morphology has recently been observed for similar mixtures.⁶

Alternative PDLC systems with lower LC weight fraction, however, exhibit a more dropletlike morphology.⁹ At 76% the domains have sufficient polymer matrix between droplets to form nondistorted spherical shapes with a diameter of $0.65 \pm 0.10 \mu\text{m}$. These domains grow in a size up to $1.8 \pm 0.2 \mu\text{m}$ at 82%, at which point the spherical shape becomes distorted to a polygon/hexagon shape due to the close packing of the domains. At this fraction we can clearly observe that each domain is surrounded in the plane by an average of five to six other domains. Above 82%, the domains become sufficiently large compared to the wavelength of light that the visible scattering cross section is too small for display applications.

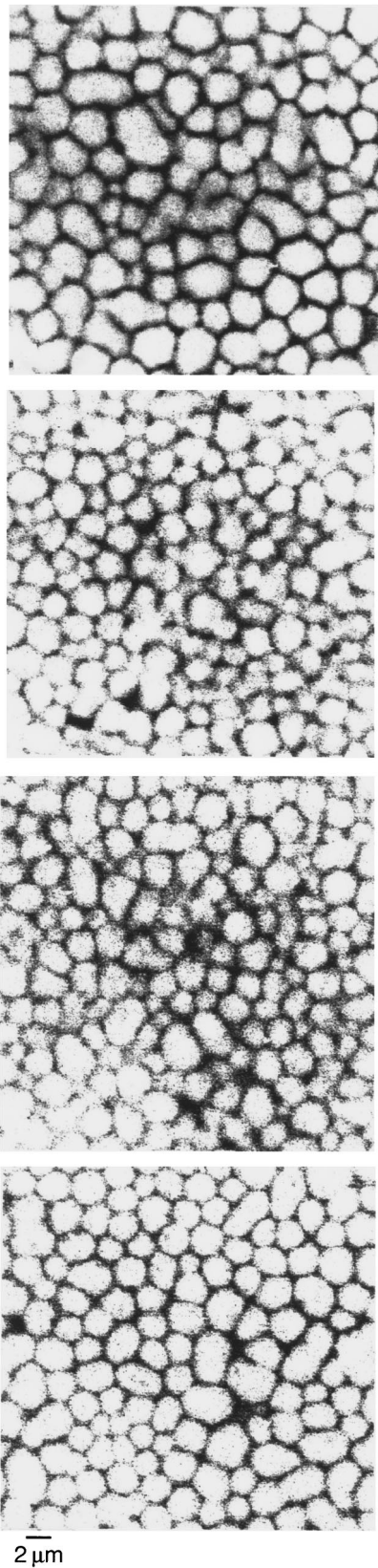


FIG. 2. Confocal visible microscopy scan through the entire thickness of the $10\ \mu\text{m}$ PDLC cell in order from top to bottom of ITO-covered glass/PDLC interface, $3\ \mu\text{m}$, $6\ \mu\text{m}$ deep, and PDLC/ITO-covered glass interface. The morphology away from the interface is only weakly dependent on scanning depth. The size of the picture is $32 \times 32\ \mu\text{m}^2$.

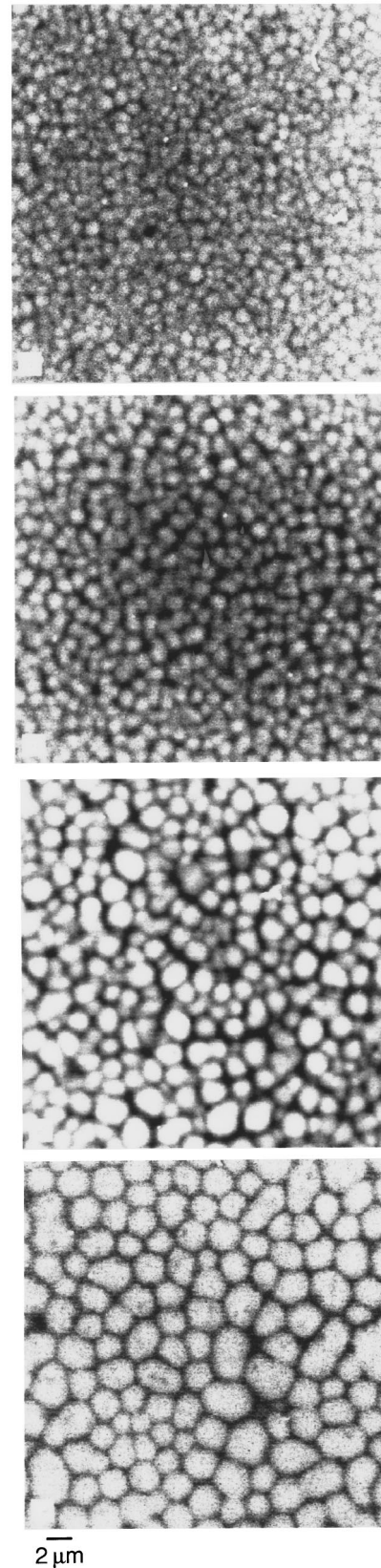


FIG. 3. Dependence of the PDLC morphology on composition at curing conditions of $24\ ^\circ\text{C}$ and $16\ \text{mW}/\text{cm}^2$. Compositions from top to bottom are 76%, 78%, 80%, and 82% LC. The droplets increase in size with increasing LC fraction.

The average droplet (domain) diameter, determined by analysis of a two-dimensional fast Fourier transform of the image, is plotted versus composition (in Fig. 6). The increase in droplet size with increasing LC fraction has been observed previously^{6,9} and can be explained by changes in the extent of polymerization at the onset of phase separation. With increasing fraction, the PDLC mixture moves closer to the phase boundary resulting in a less developed polymer matrix when phase separation occurs and more time for the LCs to form large domains. The phase separation temperature T_{ps} varies from $-5\text{ }^{\circ}\text{C}$ for 76% to $15\text{ }^{\circ}\text{C}$ for 82%. Since the cure temperature is at $24\text{ }^{\circ}\text{C}$, the 82% sample is only $9\text{ }^{\circ}\text{C}$ away from the phase transition point in comparison to $29\text{ }^{\circ}\text{C}$ for the 76% sample. The factor of 3 difference is also the factor observed in the difference in their droplet size (Fig. 6), suggesting similar linear diffusion rates for the two systems.

To further test this model, we cured the polymer at different temperatures while keeping the composition constant. For the 76% samples we observe a change in droplet size of less than $0.07\text{ }\mu\text{m}$ for samples cured at 12 and $20\text{ }^{\circ}\text{C}$, a much smaller change than the 30% decrease in the droplet size expected from the above model in which the effect of increasing temperature is to cause a larger polymer matrix to be formed at T_{ps} resulting in less time for domains to form (smaller drops). Similar results are observed for compositions 78% through 82% (summarized in Fig. 6). These results imply that the extent of polymerization at the phase separation point cannot completely account for the morphology changes. An alternative explanation would be that increasing temperature also causes a decrease in the viscosity of the polymer matrix, and therefore an increase in the molecular diffusion rate and the coalescence rate. This would result in the formation of larger droplets, offsetting the smaller droplets expected due to the increased distance from the phase separation point. We note, however, that this is an overly simplistic picture, and that there are several other factors, such as surface tension, LC anchoring energy, and the nucleation mechanism itself which need to be taken into account for a complete understanding of the morphology.

Our resolution at 76% is too low to directly observe coalescence; however, at 82% composition, the larger droplet size permits a more detailed study of changes in morphology as shown in Fig. 4. We can identify three regions in temperature phase space delineated by a threshold temperature T_{th} (Fig. 1). At low temperatures ($T_{ps} < T < T_{th}$) represented by the top panel of Fig. 4, we observe no coalescence and a uniform sponge-type texture forms. As before, very little change in the domain size occurs. In the second panel the aggregation or coalescence of the droplets can be observed at $38\text{ }^{\circ}\text{C}$. We define the temperature range at which this coalescence starts to be observed as T_{th} . For $T \sim T_{th}$, the polymer matrix freezes before the coalesced droplets can form spherical droplets, leading to elliptical shaped droplets and subsequently large moments of inertia (Fig. 6). At $48\text{ }^{\circ}\text{C}$, $T \gg T_{th}$, the matrix viscosity is sufficiently reduced that the coalesced droplets have sufficient time to relax and form larger, more spherical, droplets, as seen in the bottom panel of Fig. 4. This same effect is observed at 78% and 80% with

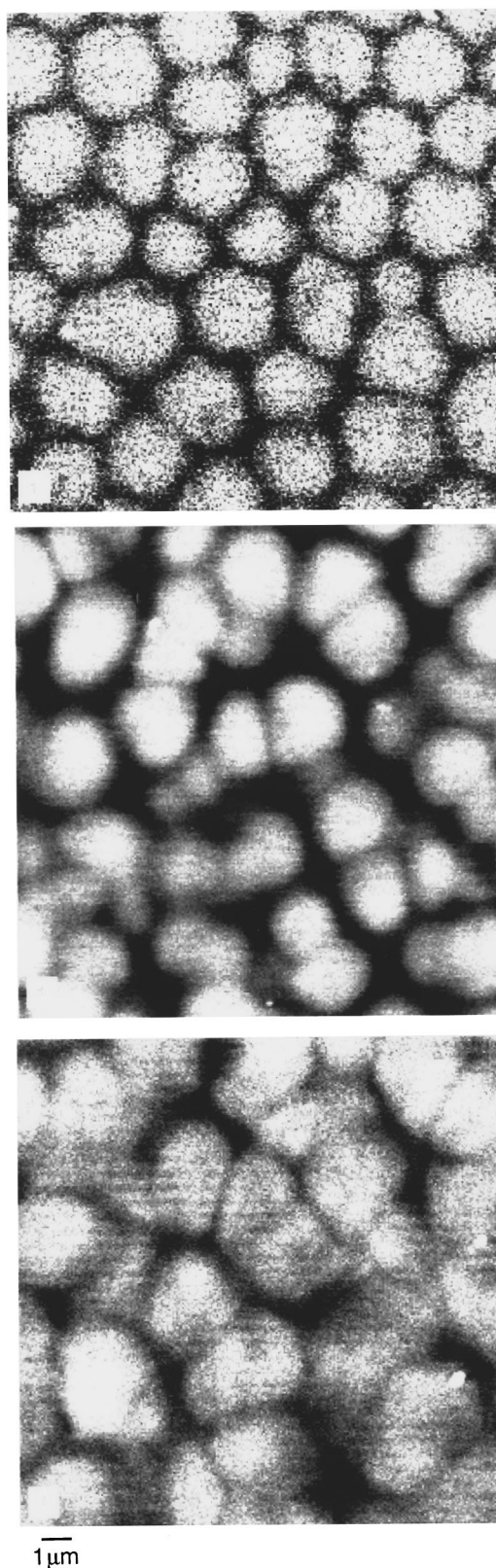


FIG. 4. Dependence of the PDLC morphology on UV cure temperature at 82% LC and 16 mW/cm^2 . Cure temperatures from top to bottom are 24, 38, and $48\text{ }^{\circ}\text{C}$. Coalescence of the droplets starts to occur near $38\text{ }^{\circ}\text{C}$ with larger droplets forming at higher temperatures. Droplet size is only weakly dependent on UV cure temperature below $40\text{ }^{\circ}\text{C}$.

T_{th} decreasing with lower LC fractions. This effect is more difficult to observe for the smaller droplet size, and our measurements indicate that the elliptical droplets form at $30\text{ }^{\circ}\text{C} <$

$T_{th} < 36\text{ }^\circ\text{C}$ for 80% and $24\text{ }^\circ\text{C} < T_{th} < 31\text{ }^\circ\text{C}$ for 78%, roughly $25\text{ }^\circ\text{C}$ above T_{ps} (Fig. 1).

Last, we vary the speed at which the phase separation line is approached by varying the UV power at fixed temperature and composition. The results for 80% composition, cured at $24\text{ }^\circ\text{C}$, are shown in Fig. 5(a), where the cure power has been changed by a factor of 1000. The droplet size, shown in Fig. 6, increased substantially with decreasing cure power below 8 mW/cm^2 . The average time for phase separation increased from a few seconds for 16 mW/cm^2 exposure to above 10 s for $23\text{ }\mu\text{W/cm}^2$ exposure. The extent of the polymer matrix at phase separation is not affected by the polymerization rate; nonetheless, the lower UV cure rate results in a slower freezing of the PDLC once phase separation is induced, allowing more time for the LC to form larger domains as observed. If we repeat the experiment in the regime where $T > T_{th}$, then the coalesced drops form larger spherical drops as expected.

Typically, the morphology that subsequently forms depends on the difference between the diffusion rate and the polymerization rate, unless the diffusion is limited by the cell dimensions. In the bottom section of Fig. 5(a), a vertical scan through the entire $13\text{ }\mu\text{m}$ PDLC shows that at the lowest exposure the cell is still two to three LC droplet layers thick. The molecular diffusion has not been significantly limited by boundary effects, and the droplet size is determined by the diffusion rate, and the shape of the droplets (distorted-pentagon and hexagon) is determined by the packing. This is not the case for the 82% composition cured at $24\text{ }^\circ\text{C}$ is shown in Fig. 5(b) where the scale on the bottom figure is 2.5 times the top scale. Here, the vertical scan shows that the layer is less than one droplet thick. As such, the droplets grow to the size of the gap at which point they start to coalesce. The ‘‘donut-type’’ structure that occurs for the $23\text{ }\mu\text{W/cm}^2$ cure presumably results from trapped polymer between coalesced neighboring droplets.

DISCUSSION

Several studies have shown that the morphology of a PDLC strongly affects the electro-optic properties.^{6,7,9} Expressions for such effects can be derived from equations relating the elastic energy density for the LC orientation to the frequency-dependent electric-field energy density inside a uniform dielectric sphere, yielding a relation for the voltage required to turn the cell ‘‘on’’ (transparent) V_{on} and the time it takes to turn the cell off τ_{off} of

$$V_{on} \sim d/R(L^2 - 1)^{1/2}(4\pi K/\Delta\epsilon)^{1/2} \quad (1)$$

and

$$\tau_{off} \sim \gamma R^2/[K(L^2 - 1)], \quad (2)$$

where R is the average droplet radius, $L = R_2/R_1$ where R_2 and R_1 are the major and minor radii of an elliptical drop, d is the cell gap, γ is the rotational viscosity, and K and $\Delta\epsilon$ are the elastic constant and the dielectric anisotropy of the LC, respectively.^{10,11} Decreasing R causes an increase in the surface anchoring energy of the LC such that more voltage is needed to switch the LC. When this voltage is removed, this same energy will cause the LC to switch back to its original

state faster. Elliptical droplets ($L > 1$) switch at higher voltages because they favor a preferred orientation that the electric field must overcome, but by the same argument they will also switch back to their original state more quickly once the field is removed.

We have measured the electro-optic properties of our cells to understand the effect the morphology has on these properties in light of the above theories. The dependence of the switching voltage on the inverse droplet radius $1/R$ as a function of changing UV power and composition is graphed in Fig. 7. For higher compositions and voltages, the dependence is linear as expected from Eq. (1) (assuming constant L); however, we clearly observe that the switching voltage does not depend on R over certain ranges of composition and temperature. In addition, V_{on} does not depend on UV curing power, even though R increases significantly. There exists a minimum V_{on} , $5.0 \pm 0.4\text{ V}$ for a set gap size of $8.5\text{ }\mu\text{m}$ and $7.0 \pm 0.4\text{ V}$ for a set gap size of $11\text{ }\mu\text{m}$, which occurs at low enough temperatures regardless of the drop size. We note that when the droplets are spherical, i.e., $L = 1$, Eq. (1) approaches zero; our morphology measurements indicate that the droplets remain very close to spherical in PDLC cells exhibiting minimum switching voltage. This result suggests that a complete equation for V_{on} would require an additional term that must depend on the intrinsic properties of the LC, such as the dielectric anisotropy and the elastic constant, and not on the PDLC morphology. The slight increase in V_{on} that occurs for the larger droplets (small $1/R$) is probably due to the distortion away from sphericity ($L > 1$) that occurs in the packing of the larger droplets.

The dependence on τ_{off} should be similar to V_{on} . Figure 7 shows changes in τ_{off} vs R^2 for changes in UV power and composition. We observe linear dependence over a limited composition range, but at higher compositions the switching time drops off in agreement with the slight rise in voltage. This is presumably due again to the distortion of the droplets from sphericity ($L > 1$) which occurs at the higher compositions. As before, UV power does not effect the switching voltage even though R is changing significantly. A possible explanation here would be that when $T < T_{th}$, $L \sim 1$ and Eq. (2) becomes undefined (τ_{off} approaches infinity) and another effect must limit the switching time. This effect must depend on the intrinsic properties of the LC, such as the rotational viscosity and elastic constant. The functional form of these additive terms is currently under further investigation.

The luminance (LUM) shows a fair amount of scatter over the samples studied. Nonetheless, we can still observe (Fig. 7) that the optical scattering in the off state is reduced as the droplet size becomes significantly larger than the wavelength of visible light. The peak in the luminance occurs for samples with composition around 76%–78% suggesting that the optimum drop size for back scattering of visible light is around $0.8 \pm 0.2\text{ }\mu\text{m}$, in agreement with previous findings.¹² As expected, lower UV cure powers result in a decrease in the luminance due to the larger drop size.

The droplet radius R remains roughly constant as a function of cure temperature (Fig. 6) so the dependence of the

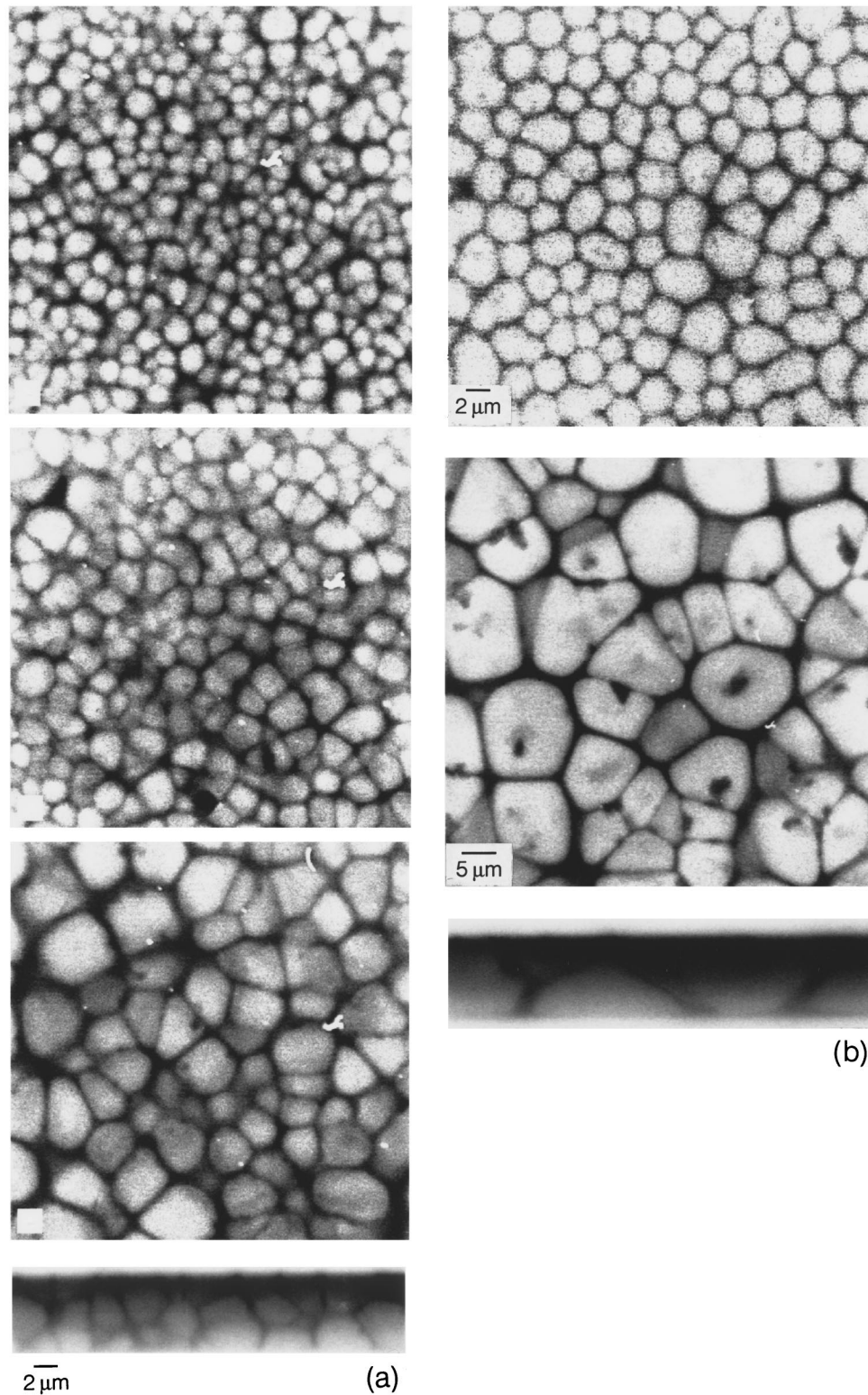


FIG. 5. Dependence of the PDLC morphology on UV cure power showing the increase in droplet size with decreasing UV cure power. (a) Changes in morphology for 80% composition and 24 °C cure temperature, with UV cure powers from top to bottom of 16, 2, and 0.02 mW/cm². (b) Changes in morphology for 82% composition and 24 °C cure temperature, with UV cure powers of 16 mW/cm² (top) and 0.02 mW/cm² (bottom). Bottom slice is a cross section of the cell showing that the droplet size is limited by the cell gap dimensions.

switching voltage, switching speed, and luminance on the temperature is determined primarily by changes in the ellipticity L due to the changes in the onset of coalescence T_{th} . In Fig. 8 we graph the electro-optic properties as a function of

temperature for 80% composition cured at 16 mW/cm², for which T_{th} starts around 30 °C. The changes in τ and V occur slightly before T_{th} , which may be due to a resolution limit in our optical observation of the coalescence. Since coalescence

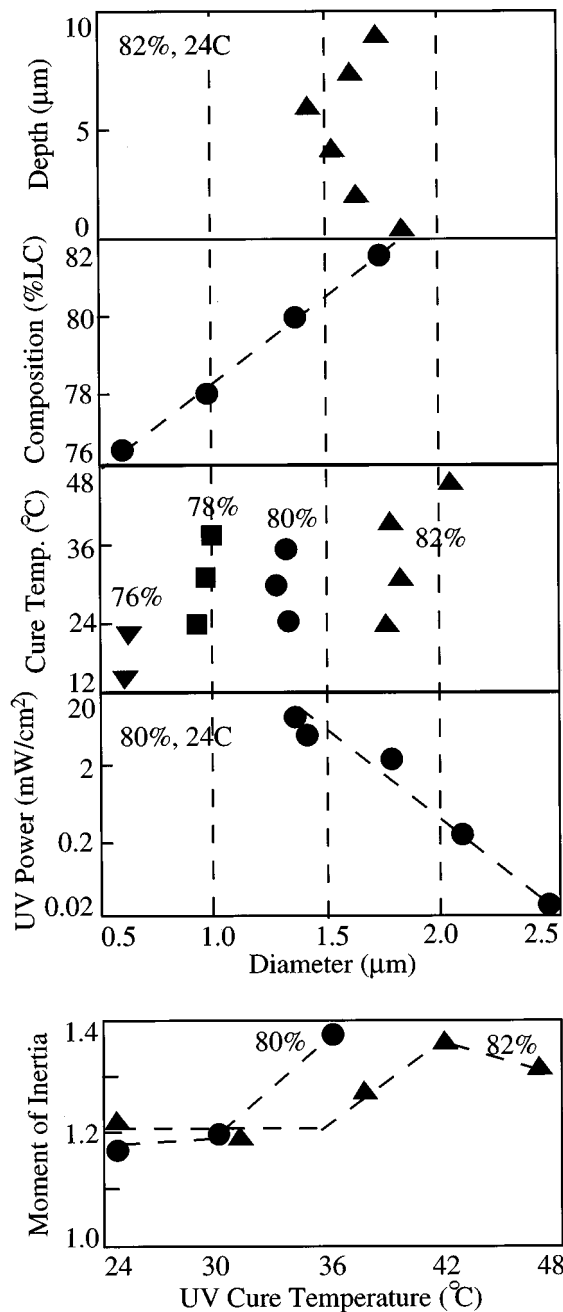


FIG. 6. From top to bottom, plots show the dependence of the LC droplet diameter on cell depth, composition, UV cure temperature for different compositions, and light intensity for a fixed composition and temperature at cure. The bottom graph shows the dependence of the moment of inertia (ellipticity of the droplets) on the UV cure temperature which results from the coalescence of droplets for two different compositions.

leads to an increase in the elliptical nature of the droplet (Fig. 6), L increases resulting in the expected increase in V_{on} predicted by Eq. (1), and the expected decrease in τ_{off} , predicted by Eq. (2). V_{on} remains constant below T_{th} as expected. The mechanism for the weak decrease of τ_{off} below the peak is unknown, but could be due to changes in the elastic constant or anchoring energy with temperature.¹³ The fastest speeds are observed for small coalesced drops (small R , large L) as predicted by Eq. (2). The observed peak in the luminance has been attributed previously to an increase in

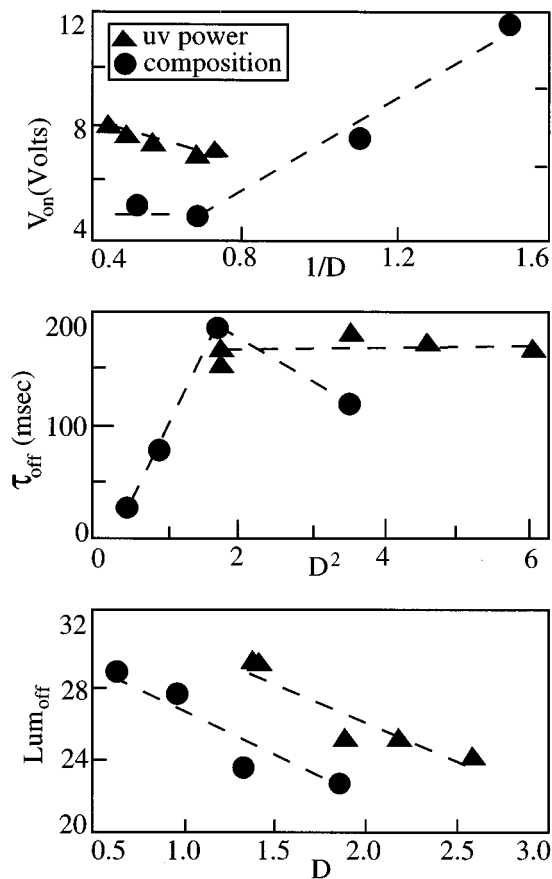


FIG. 7. Summary of the dependence of the electro-optic properties V_{on} , switching voltage; τ_{off} , the response time for switching between the transparent and scattering states; and LUM_{off} , the luminance of the scattering state, on the LC droplet radius.

the backscattering due to changes in the drop size;¹² however, we observe negligible changes in the droplet size over this temperature range. The falloff in the luminance at higher temperatures could be due to the coalescence of the drops which leads to less efficient scattering between droplets. Alternatively, there must be some additional temperature de-

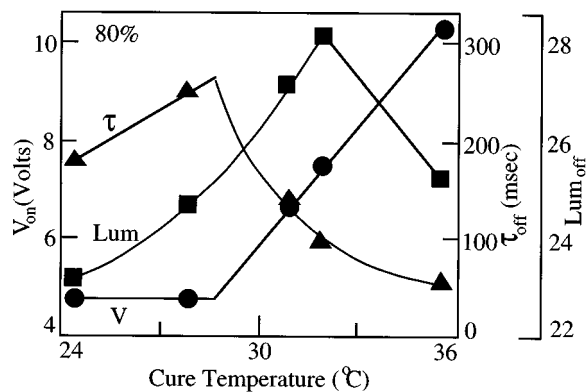


FIG. 8. Dependence of V_{on} , τ_{off} , and LUM_{off} on the UV cure temperature for 80% LC and 16 mW/cm² UV cure power. The change in properties around 30 °C marks the threshold temperature T_{th} , at which droplet coalescence starts to occur.

pendent scattering, possibly due to changes in the LC anchoring or dielectric constant, which determines the luminance.

CONCLUSIONS

We have studied the morphology and electro-optic properties as a function of varying composition, UV cure temperature, and UV cure power. We find that for the sponge-type PDLC (~80% LC fraction), the morphology is determined primarily by the rate of solidification of the polymer matrix and the viscosity of this matrix once phase separation has been initiated, with the latter property being primarily determined by the curing temperature. If this curing temperature is below the temperature T_{th} , then the morphology is determined by the nucleation mechanism and molecular diffusion, and the electro-optic properties are only weakly affected by the changes in morphology. However, if the cure temperature is increased above T_{th} , the LC domains start to coalesce resulting in substantial changes in the electro-optic properties. These results suggest that for low switching voltages and high luminance, PDLC cells should be polymerized under conditions which are below the coalescence temperature. The fastest switching times are obtained by polymerization at temperatures above the coalescence temperature.

ACKNOWLEDGMENT

We acknowledge very useful discussions with K. R. Amundson.

- ¹J. L. Fergason, Soc. Information Display Digest Tech. Papers **16**, 68 (1985).
- ²J. W. Doane, N. A. Vaz, and B. G. Wu, Appl. Phys. Lett. **48**, 269 (1986).
- ³P. S. Drzaic, J. Appl. Phys. **60**, 2142 (1986).
- ⁴R. L. Sutherland, V. P. Tondiglia, L. V. Natarajan, T. J. Bunning, and W.-W. Adams, Appl. Phys. Lett. **64**, 1074 (1994).
- ⁵T. Hirai, S. Niiyama, H. Kumai and T. Gunjima, Rep. Res. Lab. Asahi Glass Co. **40**, 285 (1990).
- ⁶K. R. Amundson, A. van Blaaderen, and P. Wiltzius, Phys. Rev. E **55**, 1646 (1997).
- ⁷J. D. LeGrange, S. A. Carter, M. Fuentes, J. Boo, A. E. Freeny, and W. Cleveland, and T. M. Miller, J. Appl. Phys. **81**, 5984 (1997).
- ⁸This result is consistent with the findings of R. Yamaguchi and S. Sato, Jpn. J. Phys. **33**, 4007 (1994).
- ⁹A. J. Lovinger, K. R. Amundson, and D. D. Davis, Chem. Mater. **6**, 1726 (1994).
- ¹⁰B.-G. Wu, J. H. Erdmann, and J. W. Doane, Liq. Cryst. **5**, 1453 (1989).
- ¹¹P. S. Drzaic and A. Muller, Liq. Cryst. **5**, 1467 (1989).
- ¹²P. Wiltzius, K. R. Amundson, and P.-Y. A. Wong (unpublished results, 1994).
- ¹³C. A. McFarland, J. L. Koenig, and J. L. West, Appl. Spectrosc. **47**, 598 (1993).